How Energy Funnels from the Phycoerythrin Antenna Complex to Photosystem I and Photosystem II in Cryptophyte *Rhodomonas* CS24 Cells

Chantal D. van der Weij-De Wit,[†,||] Alexander B. Doust,[‡,||] Ivo H. M. van Stokkum,[†] Jan P. Dekker,[†] Krystyna E. Wilk,[§] Paul M. G. Curmi,[§] Gregory D. Scholes,[‡,*] and Rienk van Grondelle[†,*]

Department of Physics and Astronomy, Faculty of Sciences, Vrije Universiteit, De Boelelaan 1081, 1081 HV Amsterdam, The Netherlands, Lash Miller Chemical Laboratories, 80 St. George Street, the Institute for Optical Sciences and Centre for Quantum Information and Quantum Control, University of Toronto, Ontario, M5S 3H6 Canada, and School of Physics and Centre for Immunology, The University of New South Wales, Sydney, N.S.W. 2052, Australia

Received: March 13, 2006; In Final Form: September 20, 2006

We report an investigation of energy migration dynamics in intact cells of the photosynthetic cryptophyte *Rhodomonas* CS24 using analyses of steady-state and time-resolved fluorescence anisotropy measurements. By fitting a specific model to the fluorescence data, we obtain three time scales (17, 58, and 113 ps) by which the energy is transferred from phycoerythrin 545 (PE545) to the membrane-associated chlorophylls (Chls). We propose that these time scales reflect both an angular distribution of PE545 around the photosystems and the relative orientations of the donor dihydrobiliverdin (DBV) bilin and the acceptor Chl. Contrary to investigations of the isolated antenna complex, it is demonstrated that energy transfer from PE545 does not occur from a single-emitting bilin, but rather both the peripheral dihydrobiliverdin (DBV) chromophores in PE545 appear to be viable donors of excitation energy to the membrane-bound proteins. The model shows an almost equal distribution of excitation energy from PE545 to both photosystem I (PSI) and photosystem II (PSII), whose trap times correspond well to those obtained from experiments on isolated photosystems.

Introduction

Over the past decade, great advances have been made in understanding the dynamics and mechanisms of light harvesting by isolated photosynthetic light-harvesting antenna complexes.[1−3] Indeed, we now possess a mature picture of how the various components of the photosynthetic apparatus that are responsible for light absorption, energy transfer, and trapping operate and how that operation is dictated by their structure.[4,5] The next step is to elucidate how all of these components work together in an intact organism. In the present work, we investigate the energy-transfer pathways that enable phycobiliprotein excitations to sensitize the electron-transfer events in photosystem I (PSI) and photosystem II (PSII) in the unicellular cryptophyte organism *Rhodomonas* CS24.

The role of phycobiliproteins as primary antenna light-harvesting proteins in cyanobacteria and red algae has been studied extensively,[6] but in the case of cryptophytes the mechanisms of excitation energy transfer and their pathways have yet to be elucidated in detail. Cryptophytes[7] have a unique pigment composition consisting of Chls *a* and *c*2, mainly the carotenoid alloxanthin, and pigments bound in just one type of phycobiliprotein. One of the most conspicuous features of cryptophytes is the location of the water-soluble phycobilin proteins at the lumenal side of the thylakoid membranes. In contrast, in cyanobacteria the phycobilisomes are bound to the stromal side of PSII.[6,8−10] *Rhodomonas* CS24 is a cryptophyte species, which exploits phycoerythrin 545 (PE545) as the primary light-harvesting antenna. PE545 is a $(\alpha_1\beta)(\alpha_2\beta)$ heterodimer whereby each $\alpha\beta$ monomer unit contains three phycoerythrobilins (PEB) and one 15,16-dihydrobiliverdin (DBV) pigment on the β and α subunits, respectively. PEB and DBV bilins absorb in the green spectral region, with absorption maxima at 545 and 569 nm, respectively, hence conferring a distinct red color to the organism. The fluorescence emission maximum is at 580 nm.

The ultrahigh-resolution structure of PE545 and interbilin energy-transfer dynamics have been described previously.[11,12] It has been shown by a measurement of the fluorescence polarization anisotropy of the isolated protein that only one of the DBV bilins in PE545 is the final acceptor of the excitation energy and is responsible for emission.[12] This may be considered surprising because the distance between the two DBV chromophores is ∼45 Å. On the basis of those studies it is therefore expected that equilibration of the absorbed excitation energy to the single red-most DBV bilin in PE545 would precede transfer of excitation energy to the chlorophyll-containing proteins bound in the thylakoid membrane. That model poses the problem that it is difficult to rationalize the light-harvesting efficiency for proteins whose emitting bilin is oriented away from the membrane.

The three main chlorophyll−protein complexes that have been isolated from the thylakoid membranes of *Rhodomonas* CS24 are PSI, PSII, and a Chl *a*/*c*2 carotenoid light-harvesting complex (LHC).[13,14] The LHC belongs to the same family of proteins as those of higher plants and *Rhodophyceae*[14,15] and

* Corresponding authors. E-mail: R.van.Grondelle@few.vu.nl; phone: (+31)20 5987930; fax: (+31)20 5987999. E-mail: gscholes@chem.utoronto.ca; phone: (+1) 416 9467532; fax: (+1) 416 9788775.

† Vrije Universiteit.

‡ Department of Chemistry, University of Toronto.

§ School of Physics and Center for Immunology, University of New South Wales.

|| Contributed equally to the work.

10.1021/jp061546w CCC: $33.50
Published on Web 11/14/2006

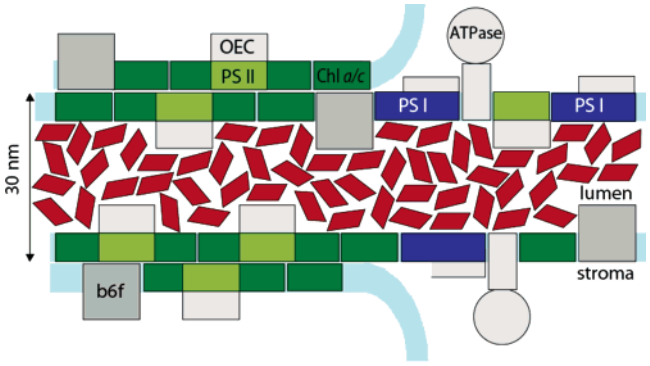

Figure 1. Scaled model of the cryptophyte thylakoid membrane. The Chl *a*/*c2* antenna (dark green) can be found in both the grana and stroma of the thylakoid membrane. The PSII core complex (light green) is largely confined to the stacked regions of the membrane of which two grana stacks are displayed on the left. The stromal part of the membrane is shown on the right and hosts the PSI complex (blue). PE545 (red) is densely packed inside the lumen. The non-chlorophyll-containing components, including the extrinsic parts of the PSII core complex involved in water oxidation, are in gray. The distance between PE545 and the chlorophylls of PSI and the Chl *a*/*c2* antenna may be short, whereas that between PE545 and the chlorophylls of the PSII core can be much larger because of the presence of extrinsic proteins.

accounts for 45% of the total Chl *a* and most of the Chl *c*2 and xanthophylls in the photosynthetic apparatus. Very efficient energy transfer from Chl *c*2 to Chl *a* has been reported for *Rhodomonas* CS24.[14] The thylakoids of *Rhodomonas* show some stacking and segregation of PSI and PSII, as in higher plants, but have a wider lumenal space.[16−19] A model of the organization of the thylakoid membranes is given in Figure 1. PSI is most likely limited to the unstacked regions, whereas the Chl *a*/*c*2 LHC may be located predominantly in the stacked regions of the thylakoids.[20,21] PE545 is densely packed in the thylakoid lumen and displays no preferential orientation, neither relative to each other nor to the membrane.[15]

In cryptophytes, the energy-transfer pathways for excitations on phycobiliproteins to the photosystems are poorly understood. Bruce et al.[22] recorded an increased contribution of phycobiliproteins to the excitation spectrum of PSII with respect to PSI in several cryptophyte algae and thus proposed preferred energy transfer from the phycobiliproteins to PSII over PSI. The same paper presents time-resolved fluorescence emission measurements at 77 K on *C. Salina*, revealing a decay time of 110 ps, for both phycobiliprotein and Chl *c*2 *fluorescence*. Lichtlé et al.[23] measured 77 K fluorescence excitation spectra of PSI and PSII, under both low- and high-light conditions. In this way, they show that spillover from PSII to PSI under high light is mediated solely by the Chl antenna of PSII and does not involve phycobiliproteins. Consequently, they suggested that the PSII antenna is composed of both phycobiliproteins and Chls, whereas PSI is provided with energy by Chls only.[24] This model strongly resembles that proposed by Mimuro et al.,[25] wherein the excitation energy from PE545 is transferred to the Chl *a*/*c*2 light-harvesting complex that is bound to PSII.

In the present work, we investigate the energy migration dynamics in intact cells of *Rhodomonas* CS24 using steady-state and time-resolved fluorescence anisotropy measurements. By fitting a specific model to the fluorescence data, we obtain the time scales by which the energy is transferred from PE545 to the Chls in the membrane. Contrary to a single-emitting DBV bilin in isolated PE545,[11] all of the peripheral bilin chromophores in PE545 appear to be viable donors of excitation energy to the photosystems in intact organisms.

Materials and Methods

Algal cells of *Rhodomonas* (formerly *Chroomonas*) CS24 species were cultivated in modified "Fe" medium[26] at 20 °C under constant low-light illumination (12 V fluorescent tubes, 300 lux at 0.3 m) and continuous aeration. Aquarium pumps are used to guarantee the air supply, and aquarium lamps provide the low-power white light throughout the entire growing process. Contamination was prohibited by filtering the medium with 0.22 μm paper filters and the air supply with a cotton filter. The algae were sealed in 1 L glass bottles and sent from Sydney to Amsterdam in darkness. It has been shown that cryptophyte cultures will continue growth for a short time in complete darkness.[27] Upon arrival in Amsterdam, the cells were subjected to normal growth conditions again. To confirm the state of health of the algae, it was seen that the absorption spectrum of the algae compared well with the absorption spectrum of the algae that was taken in Australia prior to shipment. During the experimental period, the algae were kept illuminated at constant temperature and the bottle was shaken daily to ensure sufficient air supply.

Absorption spectra were recorded using a Perkin-Elmer Lambda 40 UV/vis spectrometer. Fluorescence emission and excitation spectra were recorded on a Jobin Yvon Fluorolog-3-11 fluorometer in right angle mode. Algal solutions were diluted with double-deionized water to an optical density of 0.05 cm^{-1} for fluorescence measurements. For the 77 K measurements, glycerol (60% v/v) was added as a cryoprotectant and a nitrogen cryostat (Oxford) was used.

Time-resolved polarized fluorescence measurements were made using a streak camera setup that has been described previously,[28] including details on the data acquisition and analysis. Briefly, algal samples (2 mL, $OD_{680} \approx 0.25$ cm^{-1}) were injected into a 1 mm quartz cell and flowed continuously using a peristaltic pump (Watson Marlow, 313S) and cooled to 16 °C. Pulses (150−200 fs) at 562 nm were generated using a Ti:sapphire laser (VITESSE, Coherent), a regenerative amplifier (REGA, Coherent), and a double-pass optical parametric amplifier (OPA-9400, Coherent) with a subsequent interference filter (562 nm, fwhm 15 nm). The repetition rate was 125 kHz, and the pulse energy was 0.8 nJ. The polarization of the excitation pulses was adjusted parallel, perpendicular, or under magic angle (54.7°) with the detection polarization using a polarization compensator (Berek). The excitation light was collimated with a 15 cm focal length lens, resulting in a focal diameter of 150 μm in the sample. Vertically polarized emission was detected through a combination of a sheet polarizer and an orange sharp cutoff glass filter under right angle with the excitation beam, using a Chromex 250IS spectrograph and a Hamamatsu C 5680 synchroscan streak camera. The streak images (see Figure 2) were recorded with a cooled, Hamamatsu C4880 CCD camera. The full width at half-maximum (fwhm) of the overall time response of the experiments was 6 ps. Samples were refreshed every 30 min, and the time between the different polarized experiments was ~2 h. Global and target analysis were applied to the data, where for the global analysis a sequential model was used, yielding evolution associated spectra (EAS), and for the target analysis a more comprehensive scheme was found to be necessary to fit the data well. Such global and target analyses have been described in detail previously.[29]

Results and Discussion

Absorption. The absorption spectra of *Rhodomonas* CS24 algae at room temperature and 77 K are shown in Figure 2. The second derivative of the 77 K spectrum (see inset) shows

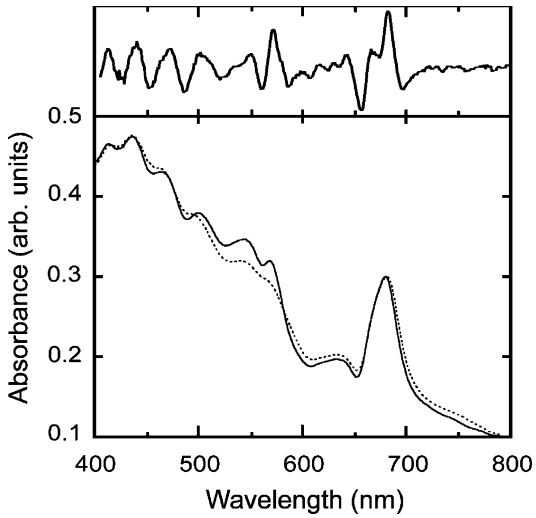

Figure 2. Room-temperature (dotted) and 77 K (solid) absorption spectra of *Rhodomonas* CS24 algal cells. The negative of the second derivative of the 77 K trace is shown at the top.

an abundance of Chl forms. On the basis of previous assignments of the spectral positions of the pigments in cryptophytes,[14,22,30,31] it was possible to assign the peak positions. The most dominant Chl *a* peak is at 681 nm, with another band at 672 nm, and the Soret band at 436 nm. Chl *c*2 has its Q_y absorption maximum at 642 nm with a Soret band at 471 nm. The carotenoids, mainly alloxanthin, absorb around 500 nm. PE545 absorbs in the region between the carotenoids and the Q_y absorption bands of the Chls. The main peaks are at 545 and 569 nm, which correspond to the PEB and DBV bilins, respectively.

Emission. Figure 3 shows the fluorescence emission spectra of the algae, both at room temperature and at 77 K at various selected excitation wavelengths, where panel b zooms in on the Chl emission. The significant PE545 emission points to the presence of a fraction of unconnected PE545 in the algae. There is a blue-shift of the emission maximum of PE545 from 585 to 583 nm upon lowering the temperature. At room temperature (dotted lines), the Chl *a* emission maximum is at 686 nm. At 77 K (solid lines), the emission maximum is split and shifted to 701 nm, with a shoulder at 684 nm. The former emission band is clearly red-shifted with respect to the expected PSII emission bands at 685 and 695 nm.[32] Because the characteristic 77 K PSI emission bands at 715, 725, and 730 nm (different cryptophytes[22]) or 735 nm (green plants) are not observed in Figure 3b, it is suggested that the 701 nm fluorescence has a contribution from PSI emission. This means that the PSI of *Rhodomonas* CS24 may not contain typical "red" chlorophylls, chlorophylls in the core and/or peripheral antenna of PSI that absorb at longer wavelengths than the primary electron donor P700.[33] Algal cells were either flushed with nitrogen or shaken thoroughly, in order to introduce oxygen in the medium, and then frozen at 77 K. In this way, P700 was dominantly reduced or oxidized, respectively. $P700^+$ does not have a specific absorption band at 700 nm but a broad absorption between 650 and 800 nm. As a result, the fluorescence emission of PSI is expected to blue-shift upon oxidation of PSI primary donor. We recorded a 4 nm blue-shift (not shown), which confirms the assignment of the red fluorescence to PSI.

For 400−480 nm excitation, an emission peak is observed at 640 nm. Upon red-shifting the excitation wavelength, the increasing contribution of a vibrational band of PE545 (at 633 nm) causes an apparent blue-shift and broadening of the 640 nm band. The emission at 640 nm is maximal upon 460 nm excitation, corresponding to Chl *c*2 absorption. The appearance of this emission is remarkable because in isolated Chl *a*/c2 complexes the Chl *c*2 delivers its excitation energy efficiently to Chl *a*,[14] Chl *c*2 emission should not be observed. Perhaps a small population of Chl *c*2 exists as a free pigment in the membrane. According to the 77 K data, an increase of PSI emission is observed upon increased selective excitation of Chl *a*, that is, shifting the excitation wavelength from 500 to 440 nm. From the steady-state data it cannot be determined whether PE545 transfers excitation directly to Chl *a* or if Chl *c*2 perhaps plays an intermediate role in the energy-transfer scheme.

Excitation. Figure 4 shows the fluorescence excitation spectra of the intact algae detected at 686 and 696 nm (at room temperature and 77 K), respectively, recording PSII and a mixture of PSI/PSII emission. Examination of these spectra clearly reveals the energy transfer from PE545 to the photosynthetic reaction centers. Unfortunately, the excitation spectra recorded at the Chl *a* emission wavelengths are not informative as to whether there is a preferred energy-transfer channel from PE545 to either of the photosystems because we do not know the relative contribution of Chl *a* absorption to the light-harvesting antennae of each photosystem. Thus, we can only conclude that PSI (696 nm) receives relatively more energy from Chl *a* with respect to PE545 than PSII (686 nm). Moreover, isolated PE545 does have some fluorescence emission at these wavelengths, for which one should correct. However, such a correction appears difficult in practice because PE545 changes spectral properties upon incorporation into the cell.

Time-Resolved Fluorescence. A two-dimensional fluorescence image of the intact algae data that was recorded under magic angle and up to 500 ps after excitation is shown in Figure 5. The emission lifetime of isolated PE545 is 2.5 ns.[34] The quenching of PE545 emission by the chlorophylls is then clear from the fast ($\ll$2.5 ns) PE545 emission decay at the blue edge of the image and the large emission rise time at 685 nm. Note that the gradual decay of PE545 emission indicates multiple lifetimes and that most of the Chl emission has decayed after 400 ps.

Global Analysis. To describe the spectral evolution, global analysis using a sequential kinetic scheme was applied to the magic angle data. Lifetimes of 3.9, 32, 107, and 411 ps were estimated, of which the evolution associated spectra (EAS) are shown in Figure 6. At its very blue edge, the PE545 emission signal is contaminated with the scatter of the excitation pulse and thus only the fluorescence from 605 nm onward is considered. To allow for a loss of PE545 emission on a time scale of 2.5 ns, probably due to a fraction of unconnected PE545, the intrinsic PE545 fluorescence lifetime was a fixed parameter in the fit. The spectrum associated with this decay time is very noisy and has less than 10% amplitude and is therefore omitted from the figure for clarity.

At time zero (the first EAS indicated by the solid line in Figure 6), both PE545 (605 nm) and Chl (689 nm) are seen to be populated. It is noteworthy to remark that this latter band is indeed absent in the emission spectrum of isolated PE545.[11] On a 4 ps time scale, the emission spectrum evolves from the solid line into the long-dashed one, showing no signs yet of energy transfer from PE545 to the Chls according to the lack of amplitude loss at short wavelengths. The gain in Chl emission at 689 nm results from the equilibration of excitation energy over the antennae of the photosystems on this time scale. The next spectral evolution occurs on a 32 ps time scale, during which a significant amount of PE545 excitations are transferred

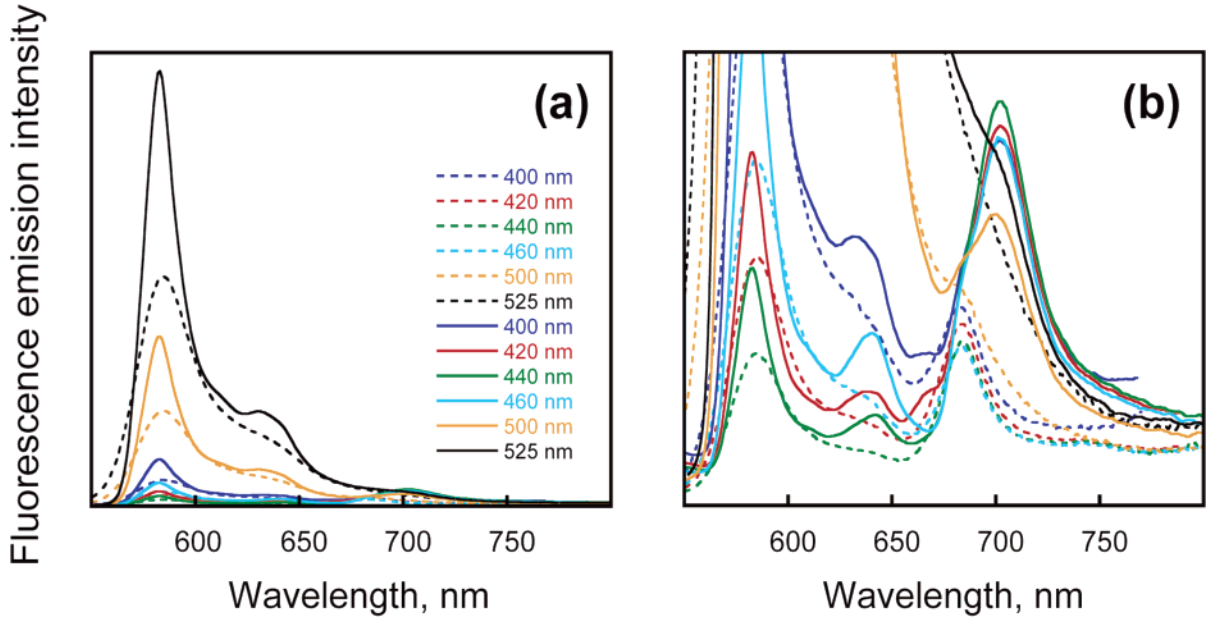

Figure 3. (a) Emission spectra of intact cells at room temperature (dotted) and 77 K (solid) at different selected excitation wavelengths, and (b) zooming in on the Chl *a* emission. PE545 emission maximum is at 585 nm (room temperature) and 583 nm (77 K). Chlorophyll emission is at 686 nm (room temperature) and 701 nm with a shoulder at 684 nm (77 K).

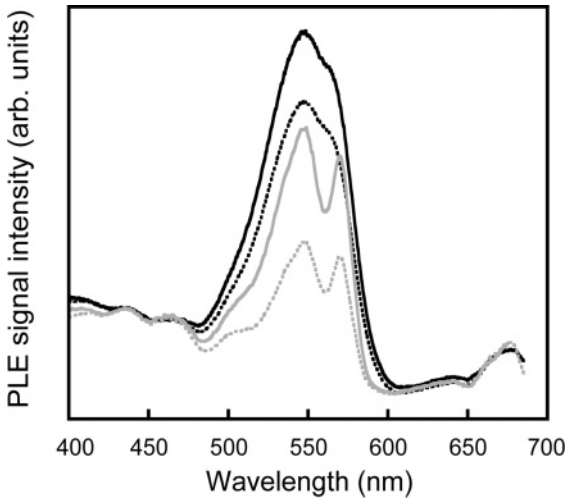

Figure 4. Photoluminescence excitation (PLE) spectra of intact cells at room temperature (black) and 77 K (gray) when monitoring emission at 686 nm (solid line) and 696 nm (dotted line). The spectra are normalized to the Chl *a* maximum at 435 nm.

to the Chls emitting at 685 nm. Then, almost all of the PE545 emission is seen to disappear on a 107 ps time scale. The final spectrum is a typical PSII fluorescence emission spectrum, with a maximum at 684 nm and an effective trapping time of 411 ps. Upon energy transfer from PE545 to the Chls, a gradual blue-shift of the Chl *a* emission is resolved, which is indicative of a shorter fluorescence lifetime for the red Chls with respect to those that emit at 684 nm, consistent with the attribution of relatively red emission to PSI and of relatively blue emission to PSII, and thus perhaps an indication for different roles played by PSI and PSII in the PE545 to Chl energy-transfer process.[35] To resolve the PE545 and Chl kinetics and to gain better understanding of this complex system, we applied a target analysis. The quality of the data limits the model complexity. In our minimal model, we distinguish three species: PE545 and two groups of membrane-bound Chls, namely, PSI and PSII, thus disregarding the spectral evolution within PE545, PSI, or PSII. Note that each EAS estimated from the magic angle data consists of different contributions from the species associated

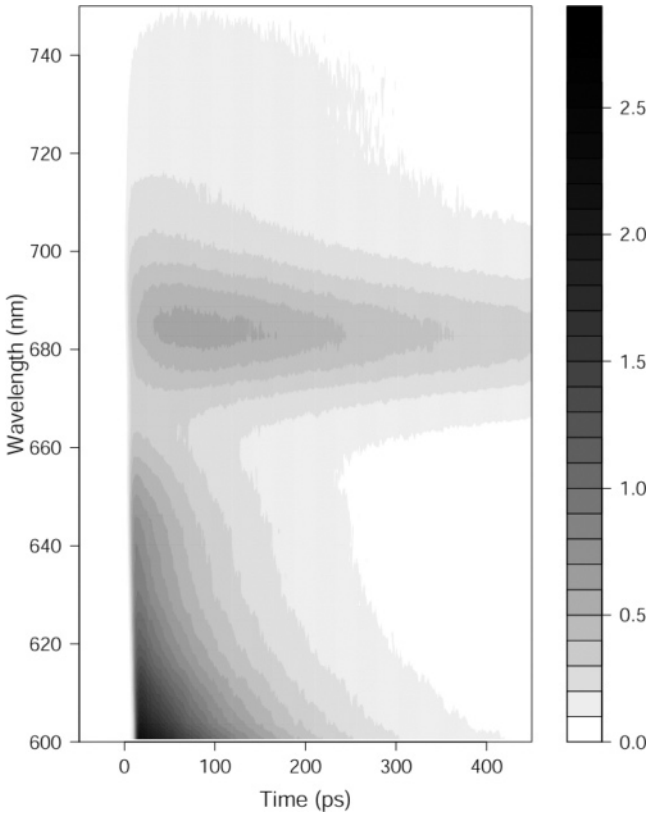

Figure 5. Filled contour plot of the time-resolved fluorescence from the intact algae. These data were recorded under magic angle with a 500 ps time base. It is seen that PE545 emission is quenched by the chlorophylls due to energy transfer.

spectra (SAS) of PE545, PSI, and PSII. Each of these three species evolves multiexponentially, and our target is to resolve realistic SAS in combination with a plausible kinetic scheme. Thereby spectral assumptions will be needed, for example, that the emission at wavelengths less than 645 nm is exclusively from PE545.

Target Analysis. Target analysis was applied simultaneously to the three polarized time-resolved emission datasets. The

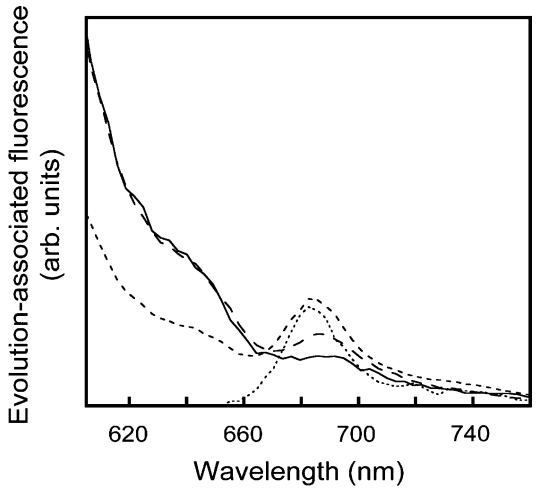

Figure 6. Evolution associated spectra of *Rhodomonas* CS24 algae upon 562 nm excitation according to the results of the global analysis. The lifetimes of the states in this sequential scheme are 3.9 (solid line), 32 (long dashes), 107 (short dashes), and 411 ps (dotted line).

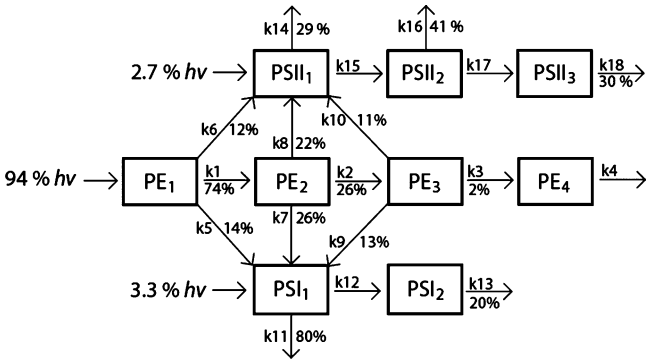

Figure 7. Target analysis kinetic scheme applied simultaneously to the three polarized time-resolved emission datasets recorded for the intact algae upon 562 nm excitation. Three species are distinguished: PE545, PSI, and PSII. PE545 emission decay is described by four decay components (PE_{1-4}), and from three of these the energy can be transferred to the Chls. From their relative amplitudes, the rates of energy transfer to the Chls can then be estimated. The fourth decay component accounts for the fluorescence lifetime of 2.5 ns. PSI and PSII decay kinetics are, respectively, described by two ($PSI_{1,2}$) and three compartments ($PSII_{1-3}$). Energy transfer from PE545 to both PSI and PSII was allowed for in a fixed ratio for each of the three transfer steps, and found to be 55:45, respectively. For simplicity, the energy transfer from PE545 to a photosystem is described by a connection to the first compartment of that photosystem. The percentages reflect the energy distribution over the different states. In PE they describe the amplitudes of the multiexponential decay, whereas in a photosystem they describe the trapping ratios. The compartment lifetimes that result from this kinetic scheme are 17, 58, 113, and 2500 ps, respectively (PE_{1-4}), 10 and 85 ps ($PSI_{1,2}$) and 48, 266, and 714 ps ($PSII_{1-3}$). The ratio of PE545/PSI/PSII initial excitation was found to be 94:3.3:2.7. The rate constants k_x and the decay associated amplitude matrix of the model are summarized in Tables 1 and 2, respectively.

kinetic scheme is illustrated in Figure 7. From the global analysis, it was found that the PE545 emission is well described by a four-exponential decay. This can be modeled by four sequential compartments (PE compartments in Figure 7). From three of these decay components, the energy can be transferred to the chlorophylls in the membrane, whereas the latter state is introduced to account for the fluorescence lifetime of 2.5 ns.[34] Next to this fixed 2.5 ns lifetime, three lifetimes and three relative amplitudes can be estimated reliably from the emission wavelengths below 645 nm, which is exclusively from PE545. The multiexponential decay of PSI and PSII can again be estimated from the data. We first assumed monoexponential decay of the excitations on both photosystems and concluded that the fit was not satisfactory. Then, for each photosystem, the number of decay phases was increased, thus increasing the number of sequential compartments, converging to a reliable, optimal fit. As a result, PSI and PSII kinetics are described by two and three compartments, respectively. Initially, using 562 nm excitation light, PE545 as well as PSI and PSII are excited. This ratio of PE545/PSI/PSII excitation was found to be 94: 3.3:2.7, which is in accordance with the absorption spectrum (Figure 2).[14] Note that this highlights how effective PE545 is in absorbing light in the green spectral region relative to the Chls. Energy transfer from PE545 to both PSI and PSII was allowed, though in a fixed ratio, for each of the three transfer steps. For simplicity, the energy transfer from PE545 to a photosystem is described by a connection to the first compartment of that photosystem. At first sight, it may seem surprising that the complex scheme of Figure 7 can be estimated. Essential to this target analysis are the shapes and amplitudes of the estimated SAS depicted in Figure 9. Our criteria for realistic SAS are that the tail of the PE545 SAS should be smooth and that both the PSI and PSII SAS look Chl-like (peaking above 680 nm, with a broad vibrational tail toward the red), with the PSI SAS red-shifted relative to the PSII SAS. As explained above, the four exponential PE545 decay resulted in three energy-transfer time scales, and from their relative amplitudes the rates of energy transfer to the Chl can be estimated. The ratio of the rates to PSI and PSII was chosen so that the areas of the PSI and PSII SAS are similar, reflecting the fact that they contain similar Chl pigments.[29] We tested many different sets of parameters to arrive at a set in which PSII receives about 45% of the energy flowing out of PE545, whereas the other 55% migrates to PSI. Representative fluorescence decay time traces and their fits are shown in Figure 8, whereas the complete data and fits are shown in Figure S1 (Supporting Information). Table 1 gives an overview of the estimated rate constants in the kinetic model of Figure 7. The fluorescence decay time of a compartment is calculated as the reciprocal of the sum of decay rates from the compartment, which are thus found to be 17, 58, 113, and 2500 ps for PE545; 10 and 85 ps for PSI; and 48, 266, and 714 ps for PSII. The excitation population of each compartment in Figure 7 can be described by a sum of exponentials over all rate constants present in the model, and as such over the estimated decay lifetimes of the nine compartments. Table 2 displays these rise time and decay associated amplitudes. For the PSI_1 compartment, we observe inverted kinetics because it is formed slowly with lifetimes of 17, 58, and 113 ps, whereas it decays very quickly with 10 ps. A further consequence is that the same observation is partially made for PSI_2, which decays with 85 ps. Similarly, inverted kinetics are observed for $PSII_1$, which is also formed with 17, 58, and 113 ps but decays with 48 ps. The 17, 58, and 113 ps components are observed to be mixed components, representing both PE545 inter- and intramolecular energy transfer as well as energy transfer from PE545 to both photosystems. Alternatively, the 10 and 85 ps lifetime components represent PSI dynamics exclusively. Similarly, the 48, 266, and 714 ps components are associated exclusively with PSII. In global analysis, excitation energy trapping on PSII was resolved on a time scale of 411 ps. In the kinetic model, this component is now split into trapping components with time constants of 266 and 714 ps. The red-shift of the 107 ps EAS with respect to that of 411 ps in Figure 6 results from the PSI fluorescence decay on the time scale of 85 ps, which is too close to the 113 ps decay of PE545

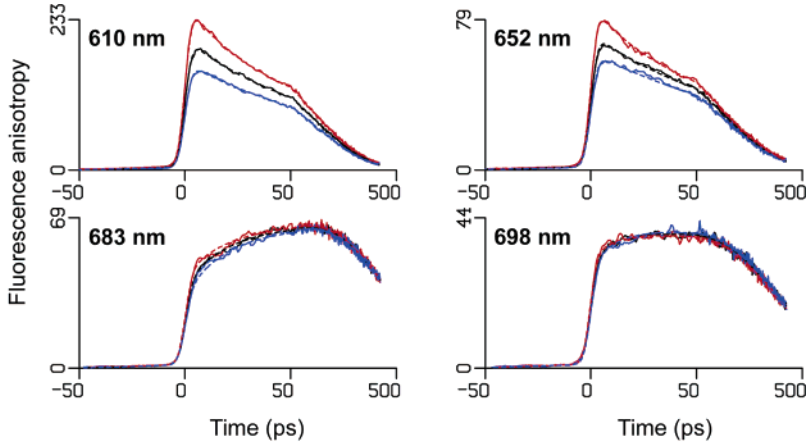

Figure 8. Selection of fluorescence anisotropy decay time-traces and their fits according to the model displayed in Figure 7. The traces at 610 and 652 nm represent the dynamics of PE545, and the traces at 683 and 698 nm represent mainly the dynamics of the Chls. Note that the time axis is linear from −50 to 50 ps and logarithmic up to 500 ps. Key to the relative polarization of excitation and detection: red, parallel; black, magic angle; blue, perpendicular.

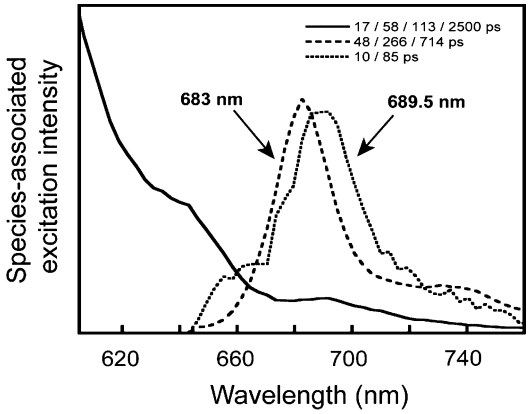

Figure 9. Species associated spectra of *Rhodomonas* CS24 upon 562 nm excitation according to the model in Figure 7. The solid line represents the emission of PE545, the dashed line is assigned to PSII (683 nm), and the dotted line is assigned to PSI (689.5 nm).

TABLE 1: Rate Constants Associated with the Target Model of Figure 7[a]

	rate, ns^{-1}		rate, ns^{-1}		rate, ns^{-1}
k1	42	k7	6	k13	12
k2	6	k8	5	k14	6
k3	0.7	k9	4.2	k15	15
k4	0.4	k10	3.5	k16	1.6
k5	8.4	k11	80	k17	2.2
k6	7	k12	20	k18	1.4

[a] Estimated relative errors are 20%.

and therefore not separated in the global analyis. Similarly, energy transfer from PE545 to the photosystems on the time scales of 17 and 58 ps are averaged to a single transfer time in global analysis, namely, 32 ps, which moreover covers the 48 ps energy trapping in the PSII reaction center ($PSII_1$). In global analysis, evolution on the short time scale, 4 ps, is observed to be specific to the Chl region. This is in agreement with the kinetic modeling, which shows fast trapping of PSI excitations on a time scale of 10 ps, whereas PE545 kinetics take place on a time scale which is a factor of 2 larger. As a consequence of the inverted kinetics of PSI_1, a rise of Chl emission is observed on this time scale.

The estimated PE545 emission spectrum is in good agreement with the recorded steady-state fluorescence emission of isolated PE545,[11] with its fluorescence tail extending far into the red. The assumed absence of spectral evolution is in agreement with earlier measured transient absorption results on PE545.[12] For PE545, fluorescence decay times of, respectively, 17, 58, and 113 ps were estimated.

The estimated PSI emission spectrum has an emission maximum at 689.5 nm (dotted spectrum); the shoulder at 660 nm is ascribed to an artifact of the fit. We resolve PSI trapping times of 10 and 85 ps, with a corresponding trapping ratio of 80:20. Such trapping times are in the range of those found in the literature for intact PSI-LHC I complexes.[5,36] The 10 ps lifetime is slightly faster than that normally observed for PSI cores, which may be partly due to the intrinsic uncertainty of this analysis, and partly may be rationalized by the absence of red Chls. The PSII spectrum (dashed) shows an emission maximum at 683 nm and was found to trap the excitation energy on three different time scales, 48, 266, and 714 ps, with a corresponding trapping ratio of 29:41:30. These trapping time scales are in accordance with literature values for PSII.[37−39] However, quite a high number of excitations are trapped on the longest time scale of 714 ps, which may be explained by the presence of a fraction of closed PSII reaction centers.[32,39]

The analysis indicates that PE545 transfers energy to both PSI and PSII. PE545 is located in the thylakoid lumen,[34] and both PSI and PSII have contact with the lumen as well as with the cytoplasmic space. The PSII core has a large mass of protein in the lumen that does not contain pigments (extrinsic proteins involved in water oxidation), which makes direct energy transfer from PE545 to the PSII core difficult. However, the PSII core probably binds peripheral Chl *a*/*c*2 antenna complexes, making PE545 → Chl *a*/*c*2 → PSII core energy transfer possible, as illustrated in the model proposed by Mimuro et al.[25] PSI has little protein mass in the lumen, making direct PE545 to PSI core energy transfer more facile. This is evidenced by the faster rate constants for energy transfer from PE545 to PSI. In addition, PSI can bind to peripheral Chl *a*/*c*2 proteins that can act as energy-transfer intermediates. In contrast to cryptophyte algae, phycobilisomes in cyanobacteria are positioned on the stromal side of the membrane, in which case PSII is in a preferential orientation for direct energy transfer because of the flat stromal surface.

Anisotropy in the emission of PE545 is obvious from the time traces in Figure 8, whereas it appears to be absent for the Chls. Spectral equilibration among bulk chlorophylls in the light-harvesting antennae of the photosystems is known to take place within several picoseconds.[6] Because that equilibration occurs approximately at the time scale of the time-resolution of the

TABLE 2: Amplitude Matrix for the Different Lifetimes Associated with the Target Model of Figure 7[a]

compartment	PE_1	PE_2	PE_3	PE_4	PSI_1	PSI_2	$PSII_1$	$PSII_2$	$PSII_3$
excitation	0.940				0.033		0.027		
10 ps					−0.095	0.022			
17 ps	0.940	−0.978	0.120	−0.002	0.064	−0.027	−0.056	0.015	
48 ps							−0.829	0.719	−0.059
58 ps		0.978	−0.691	0.028	0.037	−0.127	0.741	−0.798	0.078
85 ps						−0.056			
113 ps			0.571	−0.046	0.027	0.188	0.171	−0.492	0.104
266 ps								0.556	−0.370
714 ps									0.247
2.5 ns				0.020					

[a] Note that the sum of all amplitudes equals the excitation of each compartment.

experiment, the Chl emission anisotropy was fixed to zero in the analysis. The estimated anisotropy values should be considered as rough estimates because of limitations in the data and the modeling. An anisotropy value of 0.16 was estimated for the initial PE545 emission, which was found to decay to 0.08 on the first fluorescence decay time scale of 17 ps. No more evolution of the PE545 emission anisotropy could be extracted from the data.

In experiments on isolated PE545, it has been shown that excitation energy migrates toward the DBV bilins within a few ps.[12] Because of the limited time-resolution of the experiments shown here, we cannot exclude the possibility of competitive energy transfer at these time scales from the PEBs to the Chls in the membrane. Regarding the estimated energy-transfer time scales of 17, 58, and 113 ps in this target analysis; however, it can be assumed that the energy transferred from PE545 to the membrane Chls originates from the DBV bilins.

Table 1 shows that there is only a factor of 2 difference among the transfer rates of the three estimated PE545 transferring states to PSI (k5, k7, k9) and to PSII (k6, k8, k10). The dimensions of both the lumen[16−19] and PE545[11] thus imply that the energy transfer occurs from an angular distribution of DBV bilins adjacent to the periphery of the photosystems and their relative orientations with respect to the acceptor Chls (Figure 1). It is a property of compartmental models that such a distribution is mimicked by a small number of distinct time scales, rather than a continuum. In our case, the data are described satisfactorily by three time scales. Because PE545 is randomly oriented in the lumen with respect to the photosynthetic membrane,[14] it is thus found that energy transfer is not specific to either DBV bilin in PE545.

It is important to note that parallel to the first two PE545 lifetimes, respectively, 17 and 58 ps, the intramolecular DBV to DBV energy-transfer process in PE545 occurs. The time scale of this transfer was determined to be 20−30 ps experimentally[12] and 76 ps by Förster calculation.[40] Consequently, some anisotropy for the first two PE545 transferring states is estimated, with a larger value for the fastest decaying state.

Conclusions

On the basis of the results of the time-resolved fluorescence experiments on intact *Rhodomonas* CS24 cells, a model was put forward that describes the distribution of energy upon PE545 excitation. Excitation from PE545 ends up on the membrane-associated Chls of PSI and PSII on three estimated time scales, 17, 58, and 113 ps. We proposed that these time scales reflect an angular distribution of PE545 around the periphery of the photosystems and the relative orientations of the donor DBV bilin and the acceptor Chl. The trap times of the isolated photosystems that were derived in the model correspond well to those from experiments on isolated photosystems. The model elucidated an almost equal distribution of excitation energy from PE545 to PSI and PSII. Considering the organization of the thylakoid membrane, outlined in Figure 1, we suggested that the Chl *a*/*c*2 complex mediates the PE545 to PSII energy transfer. Furthermore, the results and the model highlighted the importance of PE545 to the organism in harvesting solar photons in the green spectral region. Importantly, it was comprehensively demonstrated that energy transfer from PE545 to the membrane Chls on the estimated time scales does not occur from the single-emitting DBV bilin only, rather both peripheral DBVs participate. It was thus suggested that spectroscopic experiments on isolated components, such as the light-harvesting antenna PE545, cannot necessarily predict its precise function in the intact species.

Acknowledgment. The research of VU-Biophysics is supported by The Netherlands Organization of Scientific Research (NWO) via the foundation of Earth and Life Sciences (ALW) and by the European Union (Grant MRTN−CT-2003-505069, Intro2). C.D.W.W. was supported by The Netherlands Foundation for Fundamental Research on Matter. The Toronto group gratefully acknowledges the following sources for funding: Natural Sciences and Engineering Council of Canada, Canada Foundation for Innovation and the Ontario Innovation Trust. G.D.S. is an Alfred P. Sloan fellow. P.M.G.C. and K.E.W. acknowledge grants from the Australian Research Council and the University of New South Wales.

Supporting Information Available: All 55 fluorescence anisotropy decay time-traces and their fits according to the model displayed in Figure 7. This material is available free of charge via the Internet at http://pubs.acs.org.

References and Notes

(1) Sundström, V.; Pullerits, T.; van Grondelle, R. *J. Phys. Chem. B* **1999**, *103*, 2327.
(2) Scholes, G. D.; Fleming, G. R. *Adv. Chem. Phys.* **2005**, *132*, 57.
(3) Fleming, G. R.; Scholes, G. D. *Nature* **2004**, *431*, 256.
(4) van Grondelle, R.; Dekker, J. P.; Gillbro, T.; Sundström, V. *Biochim. Biophys. Acta* **1994**, *1187*, 1.
(5) van Grondelle, R.; Novoderezhkin, V. I. *Phys. Chem. Chem. Phys.* **2006**, *8*, 793.
(6) MacColl, R.; Guard-Friar, D. In *Phycobiliproteins*; CRC Press: Boca Raton, FL, 1987.
(7) Bergmann, T. I. In *The Physiological Ecology And Natural Distribution Patterns of Cryptomonas Algae in Coastal Aquatic Ecosystems*; Ph.D. Thesis; Rutgers: The State University of New Jersey, 2004; p 66.
(8) Snyder, U. K.; Biggins, J. *Biochim. Biophys. Acta* **1987**, *892*, 48.
(9) Spear-Bernstein, L.; Miller, K. R. *Protoplasma* **1985**, *129*, 1.
(10) Kirk, J. In *Light and Photosynthesis in Aquatic Ecosystems*; Cambridge University Press: Cambridge, U.K., 1994.
(11) Doust, A. B.; Marai, C. N. J.; Harrop, S. J.; Wilk, K. E.; Curmi, P. M. G.; Scholes, G. D. *J. Mol. Biol.* **2004**, *344*, 135.
(12) Doust, A. B.; van Stokkum, I. H. M.; Larsen, D. S.; Wilk, K. E.; Curmi, P. M. G.; van Grondelle, R; Scholes, G. D. *J. Phys. Chem. B* **2005**, *109*, 14219.

(13) Bathke, L.; Rhiel, E.; Krumbein, W. E.; Marquardt, J. *Plant Biol.* **1999**, *1*, 516.
(14) Ingram, K.; Hiller, R. G. *Biochim. Biophys. Acta.* **1983**, *722*, 310.
(15) Hiller, R. G.; Scaramuzzi, C. D.; Breton, J. *Biochim. Biophys. Acta* **1992**, *1102*, 360.
(16) Hill, D. R. A.; Rowan, K. S. *Phycol.* **1989**, *28*, 455.
(17) Lichtlé, C.; Duval, J. C.; Lemoine, Y. *Biochim. Biophys. Acta* **1987**, *894*, 76.
(18) Toole, C. M.; Allnutt, F. C. T. In *Red, Cryptomonad and Glaucocystophyte Algal Phycobiliproteins in Photosynthesis in Algae*; Larkum A. W. D., Douglas S. E., Raven J. A., Eds.; Kluwer Academic Publishers: Dordrecht, The Netherlands, 2003; p 305.
(19) Dekker, J. P.; Boekema, E. J. *Biochim. Biophys. Acta.* **2005**, *1706*, 12.
(20) Spear-Bernstein, L.; Miller, K. R. *J. Phycol.* **1989**, *25*, 412.
(21) Lichtlé, C.; Duval, J. C.; Hauswirth, N.; Spilara, A. *Photobiochem. Photobiophys*. **1986**, *11*, 159.
(22) Bruce, D.; Biggins, J.; Steiner, T.; Thewalt, M. *Photochem. Photobiol.* **1986**, *44*, 519.
(23) Lichtlé, C.; Jupin, H.; Duval, J. *Biochim. Biophys. Acta* **1980**, *591*, 104.
(24) Sidler, W. A. In The Molecular Biology of Cyanobacteria; Bryant, D. A., Ed; *Advances in Photosynthesis*; Kluwer Academic Publishers: Dordrecht, The Netherlands, 1994; Vol. 1.
(25) Mimuro, M.; Tamai, N.; Murakami, A.; Watanabe, M.; Erata, M.; Watanabe, M. M.; Tokutomi, M.; Yamazaki, I. *Phycol. Res.* **1998**, *46*, 155.
(26) Guillard, R. L.; Ryther, J. H. *Can. J. Microbiol.* **1962**, *8*, 229.
(27) Gervais, F. *J. Phycol.* **1997**, *33*, 18.
(28) Gobets, B.; Van, Stokkum, I. H. M.; Rögner, M.; Kruip, J.; Schlodder, E.; Karapetyan, N. V.; Dekker, J. P.; van Grondelle, R. *Biophys. J.* **2001**, *81*, 407.
(29) (a) van Stokkum, I. H. M.; Larsen, D. S.; van Grondelle, R. *Biochim. Biophys. Acta.* **2004**, *1657*, 82. (b) van Stokkum, I. H. M.; Larsen, D. S.; van Grondelle, R. *Biochim. Biophys. Acta.* **2004**, *1658*, 262 (erratum).
(30) Harnischfeger, G.; Herold, B. *Ber. Dtsch. Bot. Ges.* **1981**, *94*, 65.
(31) Stoń, J.; Kosakowska, A. *J. Appl. Phycol.* **2002**, *14*, 205.
(32) Andrizhiyevskaya, E. G.; Chojnicka, A.; Bautista, J. A.; Diner, B. A.; van Grondelle, R.; Dekker, J. P. *Photosynth. Res.* **2005**, *84*, 173.
(33) Gobets, B.; van Grondelle, R. *Biochim. Biophys. Acta* **2001**, *1507*, 80.
(34) Wilk, K. E.; Harrop, S. J.; Jankova, L.; Edler, D.; Keenan, G.; Sharples, F.; Hiller, R. G.; Curmi, P. M. G. *Proc. Natl. Acad. Sci. U.S.A.* **1999**, *96*, 8901.
(35) van Grondelle, R. *Biochim. Biophys. Acta* **1985**, *811*, 147.
(36) Ihalainen, J. A.; Jensen, P. E.; Haldrup, A.; van Stokkum, I. H. M.; van Grondelle, R.; Scheller, H. V.; Dekker, J. P. *Biophys. J.* **2002**, *83*, 2190.
(37) Andrizhiyevskaya, E. G.; Frolov, D.; van Grondelle, R.; Dekker, J. P. *Phys. Chem. Chem. Phys.* **2004**, *6*, 4810.
(38) van Amerongen, H.; Dekker, J. P. In *Light-Harvesting Antennas in Photosynthesis*; Green, B. R., Parson, W. W., Eds; Kluwer Academic Publishers: The Netherlands, 2003; p 219.
(39) Van, Mieghem, F. J. E.; Searle, G. F. W.; Rutherford, A. W.; Schaafsma, T. J. *Biochim. Biophys. Acta.* **1992**, *1100*, 198.
(40) Doust, A. B.; Scholes, G. D. *J. Photochem. Photobiol., A.* **2006**, *184*, 1.